https://doi.org/10.1016/j.colsurfa.2019.124101

Breakdown mechanisms of oil-in-water emulsions stabilised with Pluronic F127 and co-surfactants

Mwamb A. Kabong[a], Walter W. Focke[a,*], Elizabeth L. Du Toit[a], Heidi Rolfes[a], Shatish Ramjee[a]

[a]*Institute of Applied Materials, Department of Chemical Engineering, University of Pretoria, Private Bag X20, Hatfield 0028, South Africa*

Dedicated to the memory of Tharwat F. Tadros.

Abstract

Pluronic F127 is an amphiphilic, water-soluble triblock copolymer with structure $EO_{100}PO_{69}EO_{100}$. Oil-in-water (1:1 by volume) emulsions were stabilised with 3.5 mM F127 together with 10 mM C12E4 or 50 mM CTAB or 60 mM SDS. Emulsion stability was evaluated as a function of oven ageing at 60°C. This was done by tracking changes in the droplet size distribution and in the shear viscosity as a function of time. The particle size distributions started out as bimodal. All the emulsions featured very high initial viscosities and strong shear thinning behaviour. The emulsion prepared with 10 mM C12E4 as cosurfactant was stable. The particle size distribution did not change even after 48 days oven ageing at 60°C. The other two emulsion broke down over time due to coalescence. The droplet size distributions shifted to larger diameters. The shift was gradual for SDS-based emulsion suggesting droplet coalescence via binary droplet interactions. In contrast, on ageing the CTAB emulsion developed an additional population of significantly larger droplets. This is consistent with a coalescence mechanism entailing local break down of large droplet aggregates to yield much larger droplets. The observed viscosity vs. shear rate trends and the effect of ageing on the emulsion viscosity supports this interpretation.

Keywords: Surfactant; emulsion; stability; Pluronic F127; coalescence

---

E-mail: walter.focke@up.ac.za

Graphical abstract

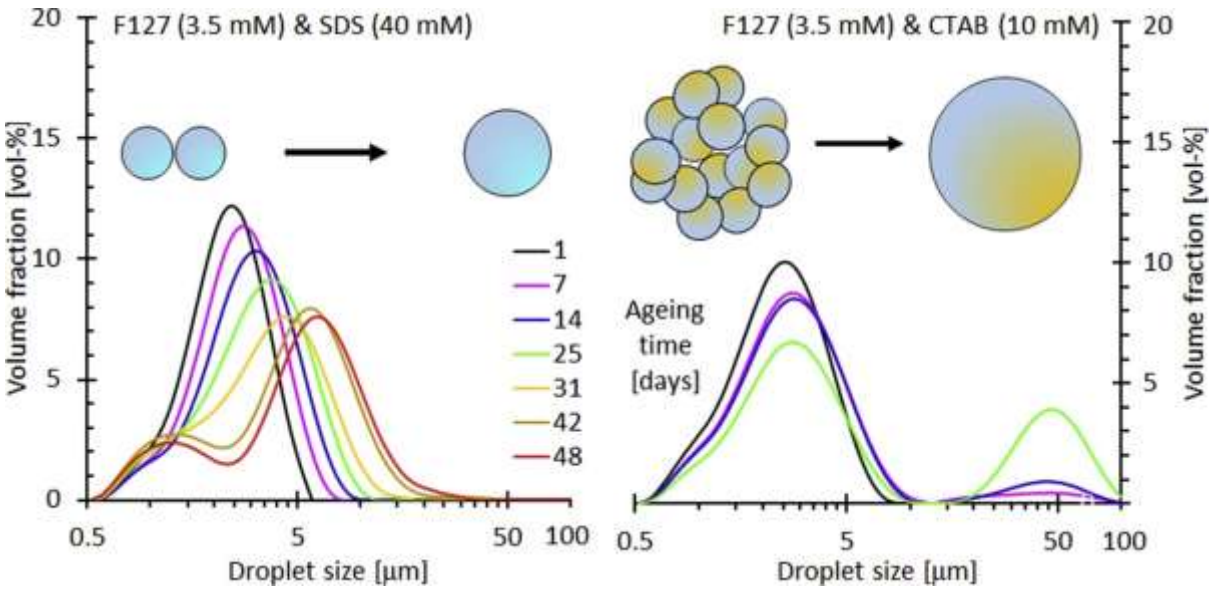

1. Introduction

The amphiphilic, water-soluble triblock copolymers of the type poly(ethylene oxide)-block-poly(propylene oxide)-block-poly(ethylene oxide) ($EO_xPO_yEO_x$) are non-ionic macromolecular surface-active agents. They are commercially available under the trade names Pluronics and Poloxamers [1]. A wide range of desirable amphiphilic properties are achievable by varying the molecular architecture, i.e. the molecular weight and the PPO to PEO composition ratio [2]. Consequently, these copolymers can meet diverse requirements in applications requiring detergency, dispersion stabilization, foaming, emulsification, lubrication, etc. [3]. Often the block copolymers are employed in combination with conventional surfactants [4].

At elevated temperatures in aqueous medium, the block copolymers aggregate into thermodynamically stable spherical assemblies, i.e. micelles. The micelle structure comprises a core containing the hydrophobic PPO blocks that is surrounded by a corona of strongly hydrated PEO blocks [5, 6]. In reality, the situation is significantly more complex. The segregation between the core and mantle is not as distinct as in conventional micelles. The core may in fact contain appreciable amounts of PEO together with some water in addition to PPO [7]. Furthermore, the PEO-mantle of the micelles tends to contract with increasing temperature.

The interactions between surfactants and synthetic macromolecules are important in many industrial applications [8]. Depending on the combination of a water-soluble polymer and a surfactant, their interaction can give rise to substantial improvement in the adsorption behaviour at interfaces [8], in the solubilisation capacities of aqueous solutions [9], and in the stability of colloidal dispersion [10], etc. The presence of a non-ionic polymer in an aqueous solution of surfactants provides a thermodynamic alternative to surface adsorption and self-micellization. The polymer chains serve as nucleation sites for ionic surfactants [11]. The surfactant molecules tend to aggregate along the polymer backbone at concentration well below their critical micelle concentration (cmc). The cooperative binding of surfactant molecules to the polymer chains leads to competition between the formation of polymer-free surfactant aggregates and polymer-surfactant complexes [12]. Consequently, these polymer-surfactant interactions significantly alter the properties of aqueous solutions.

Sastry and Hoffmann [13] reviewed the interactions between different amphiphilic copolymer micelles with conventional surfactants. As expected, the effects vary depending upon the nature and molecular architecture of the copolymers as well as the head group and hydrocarbon chain length of the conventional surfactants. Both anionic and cationic surfactants (in micellar or molecular form) interact with the associated and non-associated forms of the copolymer chains [14]. The onset of the interaction occurs at the critical aggregation concentration (cac) well below the critical micelle concentration of the surfactant. First, the surfactants bind to the hydrophobic core of the copolymer micelles and this is followed interaction with the hydrophilic hydrated halo parts. The nature and hydrophobicity of the copolymer molecule and the length of the hydrocarbon tail and type of head group determine the extent of surfactant binding. The presence of the surfactants suppresses the micellization of the $EO_xPO_yEO_x$ copolymers and even prevent it at higher concentrations.

The Pluronics strongly interact with conventional anionic and cationic surfactants, but less so with the neutral surfactants [15, 16]. Hecht and Hoffmann [4] characterised binary mixtures of Pluronic F127 ($EO_{100}PO_{69}EO_{100}$) with SDS and cetyltrimethylammonium bromide (CTAB). The strong binding of SDS to Pluronic F127 molecules was confirmed by surface tension, static and dynamic light scattering, electric birefringence and differential scanning calorimetry results. As surfactant is added, the SDS associates with the Pluronic F127 micelles causing a

reduction in their size. Initially, the surface activity derives from the mixed F127/SDS complexes until the SDS binding saturates and SDS forms its own micelles.

Surface tension data is often reported [4, 15, 17-21] but there is a dearth of interfacial tension results [5]. Therefore, the present communication reports on the association of Pluronic F127 with SDS (anionic), CTAB (cationic) and C12E4 (non-ionic) as inferred from both water-air surface tension and interfacial tension measurements at the water-mineral oil interface respectively. The objective of these measurements was to gain a more detailed understanding of interaction between non-ionic triblock copolymer with both ionic and neutral surfactants.

Ultimately, oil-in-water emulsions stabilised with binary combinations of F127 and the surfactants were prepared. These emulsions are ubiquitous in the food, pharmaceutical and chemical industries. The aim was to investigate emulsion stability and emulsion breakdown mechanisms when F127 is used in combination with different surfactant types. For this purpose, particle size distributions, viscosity vs shear rate flow curves and micrographs of the ageing emulsions were used as complimentary techniques.

2. Materials and Methods

2.1 Materials

Sodium dodecyl sulphate (SDS) (95% purity) and cetyltrimethylammonium bromide (CTAB) (99% purity) were purchased from Sigma-Aldrich. Rebound Chemical supplied tetraethylene glycol monododecyl ether (C12E4). BASF donated Pluronic F127 (poly(ethylene oxide)$_{100}$-poly(propylene oxide)$_{69}$-poly(ethylene oxide)$_{100}$ of average molecular weight 12600 g·mol^{-1}). Light mineral oil (density 0.838 g·cm^{-3}) was purchased from Fourchem (Pty) Ltd. Analytical grade sodium phosphate (Na_3PO_4) (95% purity), supplied by Associated Chemical Enterprises, was used in the preparation of all emulsions. All chemicals were used as received without further purification.

2.2 Methods

2.2.1 Surface tension measurements

Surface and interfacial tension measurements were performed at 20°C on a Kruss model DSA100 instrument using the pendant drop method. Calibrations were done with pure water (taking σ = 72 mN·m^{-1}) and assuming for the water-light mineral oil interface that the interfacial tension follows σ = 51.83 – 0.103 T/[°C] mN·m^{-1} [22]. Reported values represent averages of triplicate evaluations. All solutions were prepared by combining appropriate quantities of polymer and surfactant stock solutions. The mixtures were allowed to equilibrate at room temperature for at least 24 h before surface tension measurements were performed. Data sets corresponding to constant F127 concentrations were generated. They correspond to concentrations that were below (0.01; 0.05 and 0.10 mM) and above (3.5; 4.0 and 4.5 mM) the cmc of F127 (cmc = 3.17 mM at 20 °C [6]). At each F127 level, the concentration of a cosurfactant was varied in attempts to cover the range from the monomers to micelles.

2.2.2. Emulsions preparation

Mineral oil-in-water emulsions were prepared in a one-to-one volume ratio (50 vol-%). The aqueous phase contained 3.5 mM F127 and 0.37 M of Na_3PO_4. The co-surfactant concentrations were set at 30, 40, 50, 60 mM for SDS and CTAB, and 5, 10, 20 and 30 mM for C12E4. Duplicate emulsions were prepared with a Silverson L5M-A laboratory mixer. A typical procedure was as follows. The required amount of the light mineral oil was placed in a beaker and heated to approximately 70°C on a hot plate. A previously prepared aqueous phase was stirred at 3000 rpm and the hot oil was added slowly over a period of about one minute. Thereafter, the mixture was agitated for another two minutes after which the stirring speed was increased to 7500 rpm and maintained for an additional ten minutes. The resulting emulsion was removed from the homogenizer. It was gently agitated with a magnetic stirrer while cooling down to room temperature.

2.2.3. Particle size distribution

Emulsion stability was evaluated by tracking the changes in the particle size distribution as a function of ageing time. Towards this purpose, duplicate sets of the emulsions were aged in

a convection oven set at a temperature of 60°C. Droplet size distribution was evaluated with a Malvern MasterSizer 3000 instrument. The refractive and adsorption indices for the continuous medium were taken as 1.33 and 0.10 respectively. The refractive index for the dispersed phase was taken as 1.52. Particle size distributions were determined immediately after the emulsion preparation and at regular time intervals afterwards.

Invariably, the emulsions particle size distributions were multimodal. In order to obtain a better picture, the cumulative form of the particle size distributions were deconvoluted using a linear combination of a series of log-logistic distributions:

$$F(d) = \sum \omega_i F_i(d) \qquad (1)$$

Here d is the oil droplet diameter and ω_i is the fractional contribution from the cumulative distribution F_i, characteristic of droplet population i.

$$F_i(d) = \left(d/\alpha_i\right)^{\beta_i} \Big/ \left[1 + \left(d/\alpha_i\right)^{\beta_i}\right] \qquad (2)$$

Equation (2) defines the mathematical form of the log-logistic distribution F_i. The median droplet diameter corresponds to α_i. The shape factor $\beta_i > 2$ is related to the spread of the droplet size distribution of population i. Large β_i values are indicative of narrow distributions.

2.2.4. Microscopy

Optical micrographs of the copolymer-surfactant stabilized O/W emulsions were captured with a Zeiss Axio Imager 2 optical microscope fitted with a digital camera. The emulsion samples were diluted before placing on a microscope slide and covering with a cover slip. The emulsion structures were resolved by differential interference contrast (DIC).

2.2.5. Rheological measurements

Rheological measurements were limited to intact emulsion samples. They were performed on a Physica MCR 301 instrument using the cone-and-plate geometry in the controlled shear rate mode. The gap was 0.051 mm and the cone angle was 1.007°. The emulsion samples were hand-shaken before measurements. The shear rate was varied from 0.1 to 1000 s^{-1}. The viscosity vs. shear rate flow curves were obtained at ambient temperature, approximately 25°C.

3. Results

3.1. Surface and interfacial tensions

The influence of the Pluronic F127 concentration on the adsorption and aggregation behaviours of SDS, CTAB and C12E4 in the aqueous phase were indirectly inferred from the results obtained for the surface tension at the water-air boundary and the interfacial tension at the water-oil interface. Figure 1 displays the experimental data obtained at 20°C for Pluronic F127 and the three conventional emulsifiers. Overall, the results are in broad agreement with literature [4] with reported cmc values for the individual surfactants and the block copolymer as follows: SDS, 8.3 mM [23], CTAB, 1.66 mM [24] C12E4, 0.064 mM [25] and F127, 3.17 mM [6]. Pluronic F127 addition decreased the surface tension more gradually when compared to the surfactants. Furthermore, the final surface tension achieved beyond the cmc was higher too.

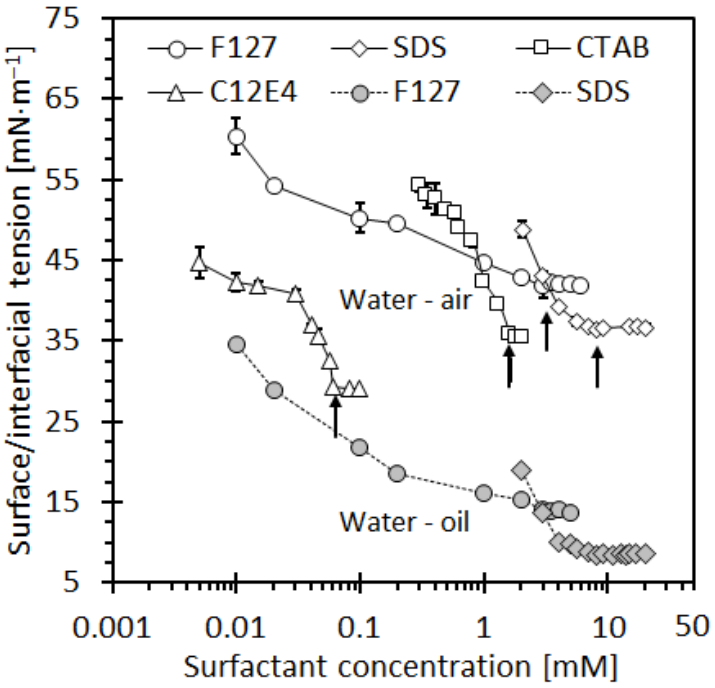

Figure 1. Surface tension (open symbols) and interfacial tension (filled symbols) results for the neat surfactants Pluronic F127, SDS, CTAB and C12E4. The arrows indicate literature-reported cmc values for each of the surface-active agents [6, 23-25].

Figure 2, Figure 3 and Figure 4 show surface tension data for binary mixtures of the surfactants with Pluronic F127. Each curve shows the effect of the surfactant concentration for fixed Pluronic F127 contents, set at concentrations below its cmc. The interactions

between Pluronic F127 and SDS are very complex and known to be strongly concentration and temperature dependent [11, 26]. The surface tension results presented in Figure 2 show the effect of SDS binding to monomeric F127. Initially, the surface activity is due exclusively to the presence of the Pluronic F127 monomers at the air/water interface. On addition of SDS, the surface tension decreases in two steps towards two separate plateau regions. The initial decrease is due to the partitioning of SDS between the bulk solution and its adsorption at the air/water interface where Pluronic F127 is also present. The critical aggregation concentration (cac) is reached at the start of the first surface tension plateau region. It corresponds to the onset of interaction between the SDS and the block copolymer. The cac is significantly lower than the cmc of pure SDS and it shows a weak dependence on the Pluronic F127 concentration. According to Li, Bao, Wang, Zhang and Xu [27], SDS binds to the block copolymer mainly through hydrophobic interactions. At saturation about six molecules of SDS bind to one F127 molecule [4] resulting in a complex "pearl-necklace" structure [11]. Beyond the first plateau, SDS accumulation at the air/water interface resumes with a concomitant reduction in the surface tension. Eventually the air/water interface is saturated and the SDS starts aggregating in the bulk. This corresponds to an extended critical micelle concentration (cmc_e). It exceeds the cmc of the neat surfactant as the block copolymer represents an alternative adsorption domain. This also explains the escalation in the SDS cmc_e with increasing F127 content.

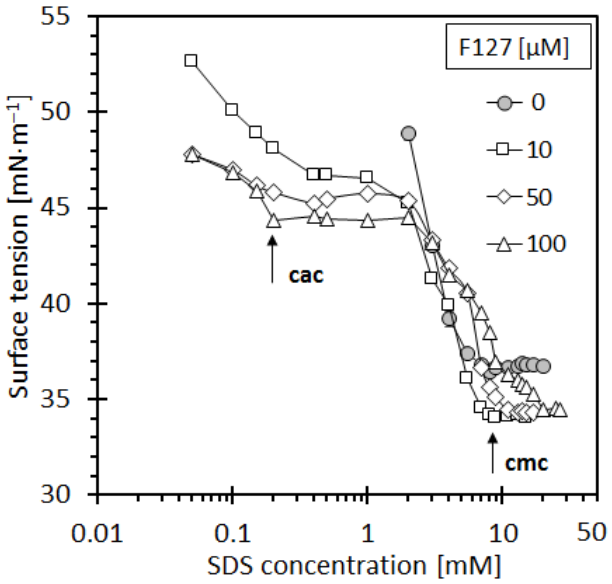

Figure 2. Water-air surface tension of binary mixtures of the surfactant SDS with Pluronic F127 as measured at 20°C. Each curve corresponds to a fixed Pluronic F127 concentration (present below its cmc).

The same pattern of association with individual block of F127 applies to CTAB and C12E4 as shown in Figure 3 and Figure 4 respectively. The initial reduction of surface tension on addition of CTAB or C12E4 was not observed. The lowest concentrations considered presently already exceeded the corresponding cac values. Surface tensions beyond cmc were similar (CTAB) and lower (for C12E4) than those of the neat surfactant solutions. The isotherms for different F127 concentrations also indicate extended critical micelle concentration (cmc_e) for these two surfactants.

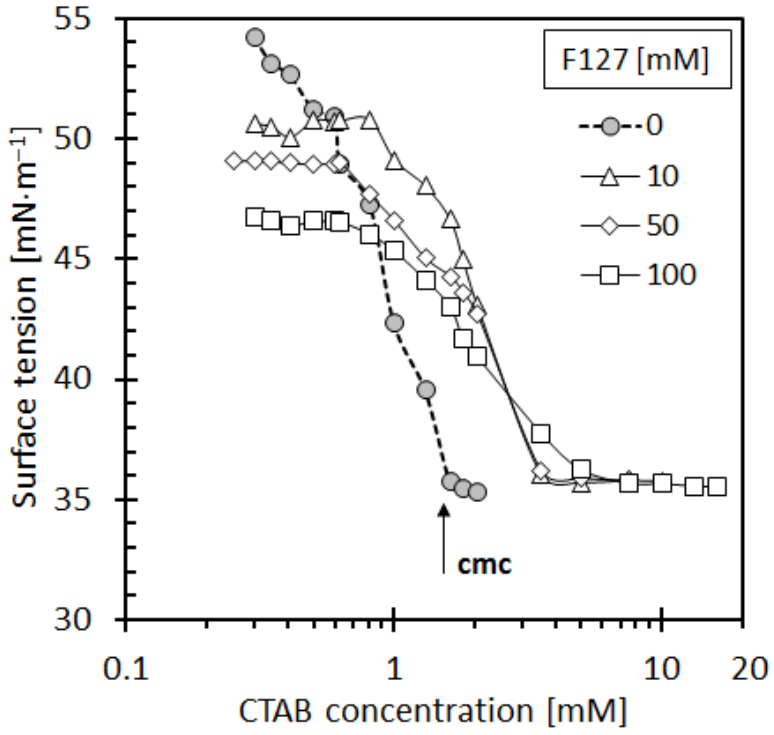

Figure 3. Water-air surface tension of binary mixtures of the surfactant CTAB with Pluronic F127 as measured at 20°C. Each curve corresponds to a fixed Pluronic F127 concentration (present below its cmc).

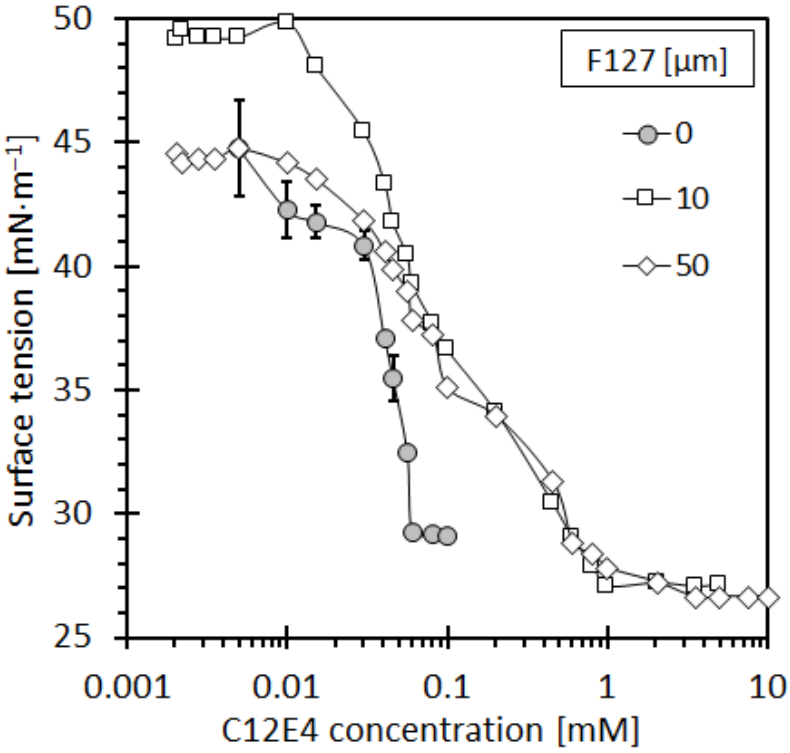

Figure 4. Water-air surface tension of binary mixtures of the surfactant C12E4 with Pluronic F127 as measured at 20°C. Each curve corresponds to a fixed Pluronic F127 concentration (present below its cmc).

Figure 5 compares surface tension data for the neat surfactants with those for binary mixtures with Pluronic F127 present just above its cmc (3.5 mM). The surface tension for the mixtures starts out at the value expected for the neat block copolymer, about 42.5 $mN \cdot m^{-1}$. Initially additions of SDS and CTAB do not affect the surface tension. At some point, well below the surfactant cmc, the surface tension suddenly increases. The surface tension passes through a maximum at a surfactant concentration roughly corresponding to the cmc value of the neat surfactant before decreasing again. This behaviour was previously attributed to the interactions between the surfactants and the block copolymer [1, 4, 11, 28]. Both SDS and CTAB bind strongly to the block copolymer suppressing the Pluronic F127 micelle formation with similar efficiency. Static light scattering (SLS) and small angle neutron scattering (SANS) measurements indicated that continuous addition of SDS systematically causes the disintegration of the F127 micelles before predominantly SDS-based micelles are formed [1, 13]. The implication is that the surfactants interfere with the micelle formation of Pluronic F127. At sufficiently high surfactant concentrations, the block copolymer micelles are completely eliminated [4]. Thereafter, the SDS or CTAB saturate the surface and form their own micelles with perhaps some of them incorporating one or more block copolymer molecules.

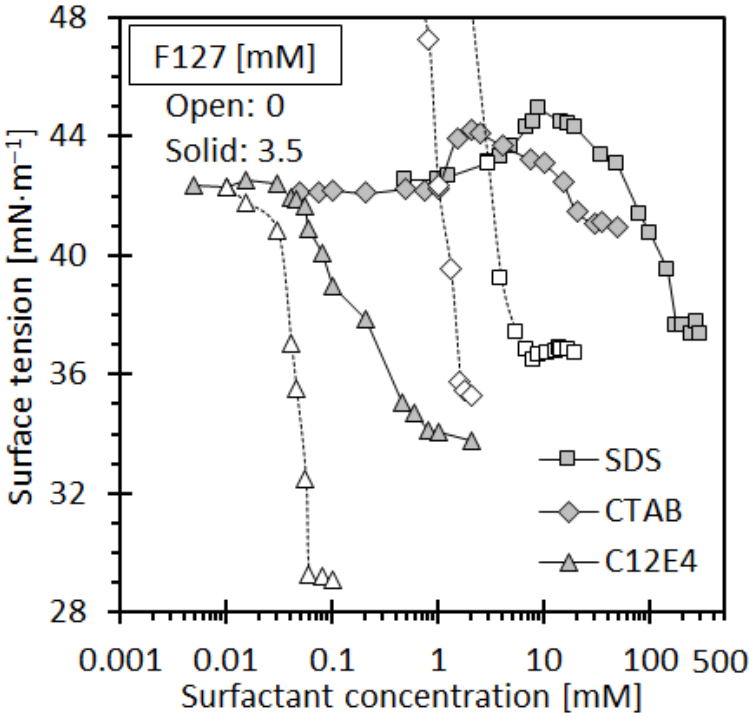

Figure 5. Water-air surface tension results obtained at 20°C for the neat surfactants (open symbols and broken lines) and for binary mixtures (filled symbols and solid lines) with the Pluronic F127 concentration set at 3.5 mM (i.e. at approximately its cmc).

The variation of surface tension with C12E4 addition differs from that of the others. The surface tension does not show an increase at intermediate concentrations. This could be due to the non-ionic surfactant forming mixed micelles with the block copolymer [29]. Both uncharged amphiphilic compounds feature hydrated EO chains in the presence of water. This may explain the ready association of C12E4 and Pluronic F127 assuring complete miscibility in the mixed micelles.

The surface tension of the mixed system started to decrease once the cmc of the neat C12E4 was exceeded. However, the reduction with added surfactant is rather gradual and it levels out at surface tension values that are higher than are obtained with neat C12E4. Nevertheless, they are lower than is attained with neat Pluronic F127. This final surface tension result is similar to that observed with CTAB. However, it differs from the situation with SDS where the ultimate surface tension values are the same.

Figure 6 shows interfacial tension results obtained at 20°C at the water/mineral oil interface. In essence, the effect of surfactant concentration mirrors the results obtained for surface

tension. At low surfactant concentrations, the interfacial tension is independent of the amounts added. However, for SDS and CTAB, the interfacial tension passes through a maximum and then drops to significantly lower values. In contrast, the interfacial tension curve for C12E4 simply shows a decrease beyond a critical value. This decrease commences at lower concentrations, occurs more gradually and levels out at higher interfacial tension values than are attained by SDS and CTAB.

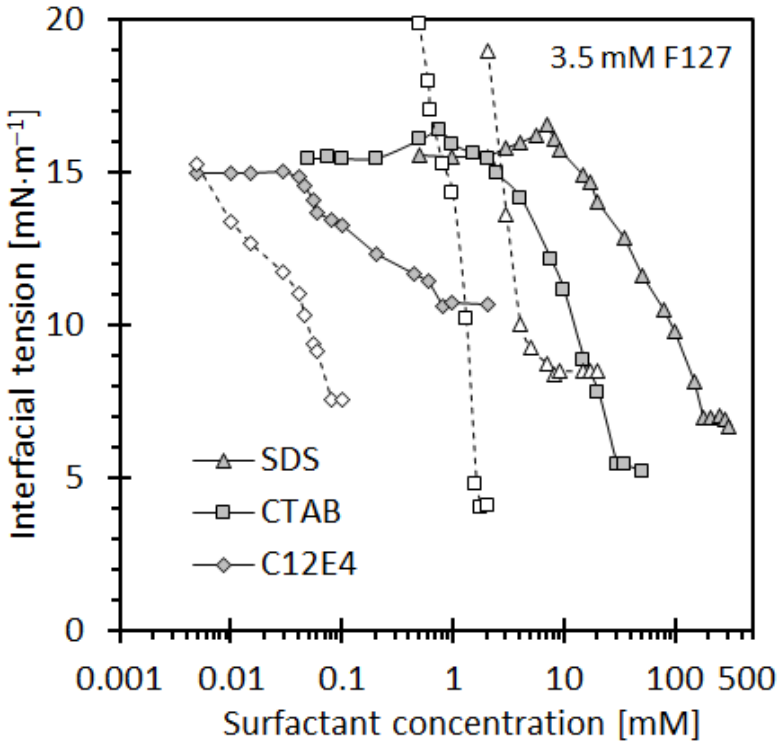

Figure 6. Water-oil interfacial tension of neat the surfactants (open symbols and broken lines) compared to results for binary mixtures (filled symbols and solid lines) with Pluronic F127 at 3.5 mM (i.e. at its cmc). Results obtained at 20°C.

3.2. Emulsion Stability

Emulsion stability was inferred from changes in the particle size distributions as a function of ageing at 60°C. Samples of the emulsions stabilised with the neat surfactants, i.e. 60 mM CTAB or 20 mM and C12E4 proved unstable breaking within one week. The 50 mM SDS on its own was sufficient to yield a stable emulsion lasting for more than 48 days. However, coalescence activity was evident from a peak shift and a third droplet size distribution evolved starting at day 30. The emulsions stabilised by combinations of surfactants and Pluronic F127 all contained 3.5 mM of the latter. Figure 7, Figure 8 and Figure 9 show typical trends for C12E4,

SDS and CTAB respectively. All the particle size distributions of the emulsions featured a "knee" at low particle size values. This is suggestive of an underlying bimodal nature even in the freshly prepared emulsions.

The PSDs of the Pluronic F127 plus C12E4 series were determined on a weekly basis. The results for 10 mM C12E4 as cosurfactant are reported in Figure 7. This emulsion was stable, as the particle size distribution did not change even after 48 days oven ageing at 60°C. Emulsions stabilised with 5, 20 and 30 mM C12E4, in addition to 3.5 mM Pluronic F127, showed similar stability. However, the emulsion made with just 1 mM C12E4 did show a steady increase in particle size over time. The mean droplet size increased from the initial value of 3.2 μm to 4.2 μm on day 40. The emulsion was broken by day 48 as evidenced by a liquid oil layer that formed on top of the liquid.

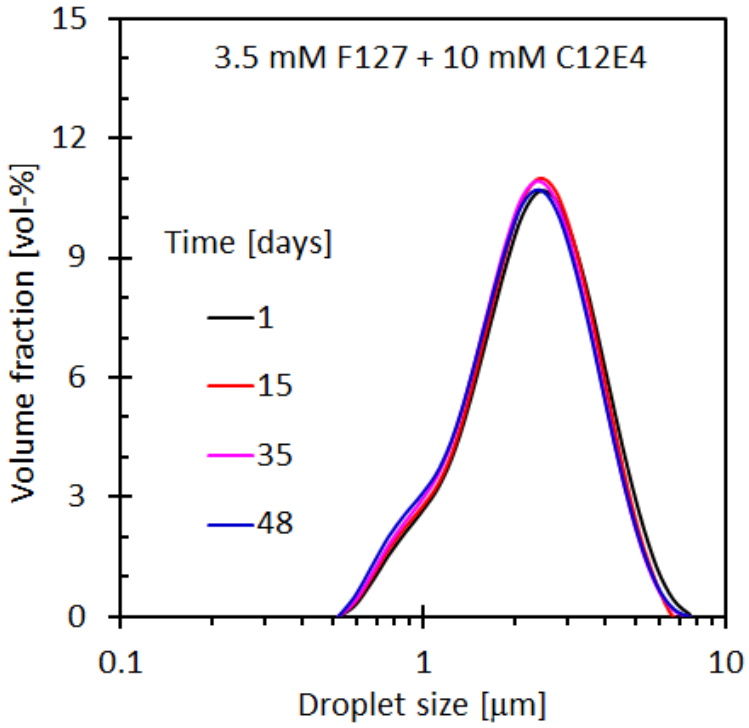

Figure 7. Evolution of particle size distribution as a function of ageing time at 60°C. The emulsion contained 3.5 mM Pluronic F127 and 10 mM C12E4.

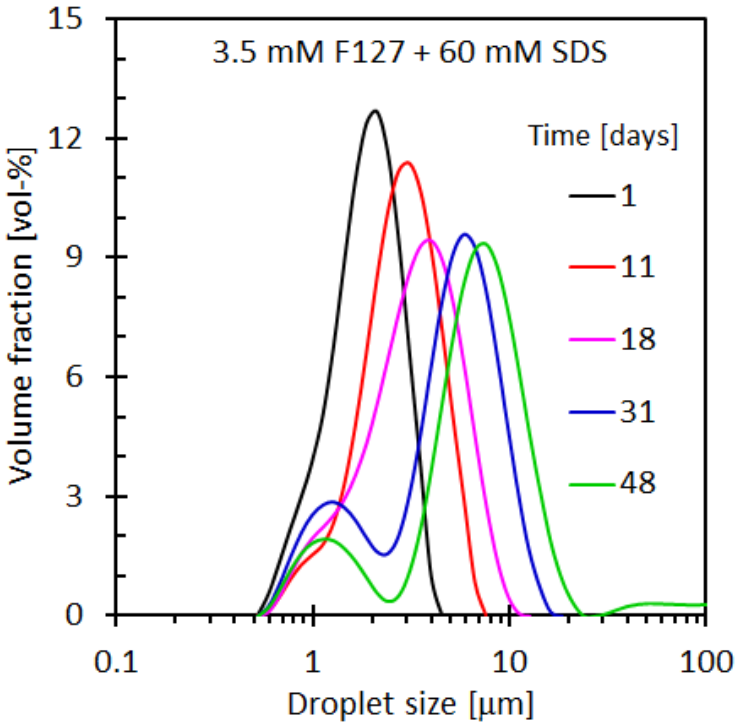

Figure 8. Evolution of particle size distribution as a function of ageing time at 60°C. The emulsion contained 3.5 mM Pluronic F127 and 60 mM SDS.

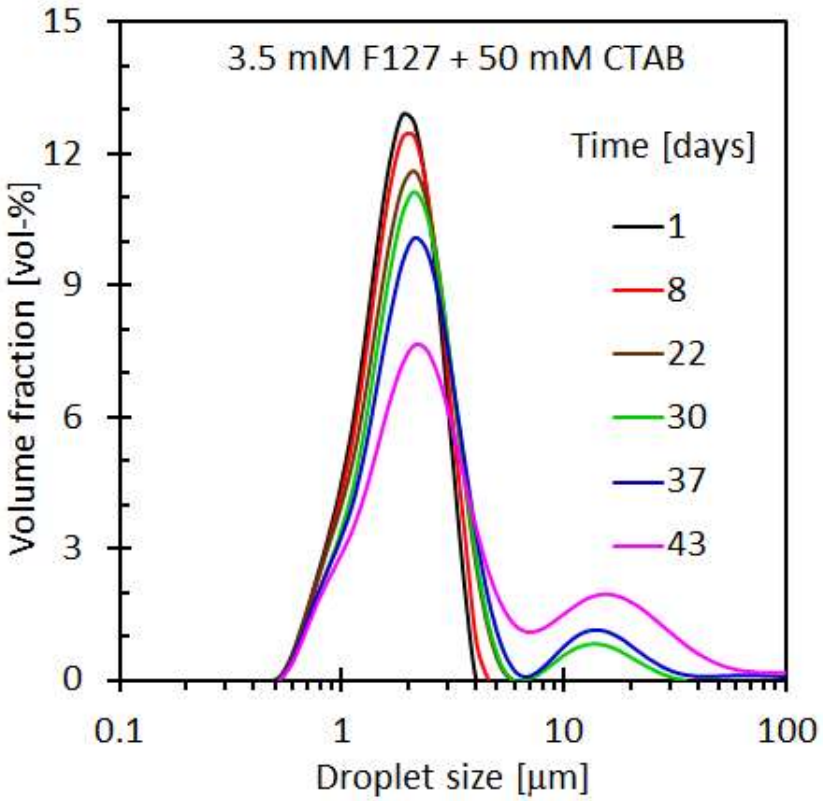

Figure 9. Evolution of particle size distribution as a function of ageing time at 60°C. The emulsion contained 3.5 mM Pluronic F127 and 50 mM CTAB.

Figure 8 and Figure 9 show that, over time, the PSDs of the SDS and CTAB stabilised emulsions developed definitive splits into two and even more droplet size distributions. The lower-range one appears to represent a population of smaller droplets (median diameter: $d_{\mathrm{m}} \approx 1.2$ μm) that maintained its size over time. However, the volume fraction of this droplet population did decrease over time. Furthermore, Figure 10 shows that the median droplet diameter for this population was nearly independent of the SDS concentration. The PSD for the larger-size droplet population of SDS-stabilised emulsions showed a steady shift towards larger particle sizes as shown in Figure 10. This behaviour is consistent with droplet coalescence as the emulsion break down mechanism. Initially the mean particle size for this group was 2.1 μm and it increased to about 6.9 after 48 days of ageing. After this ageing time, a third peak, also developed and the emulsion finally broke. This behaviour was very similar to the behaviour of the emulsion stabilised with SDS alone, i.e. it seems that the additional presence of the Pluronic F127 made little difference to the emulsion stability. This is surprising in view of the interfacial tension results presented in Figure 6 which suggest that SDS would preferentially adsorb on the non-ionic block copolymer reducing its availability to stabilise the oi-in-water emulsion.

The second peak in the PSD of the CTAB-stabilised emulsion also showed a steady, but less pronounced, shift from small (2.1 μm) to slightly larger droplet sizes (2.4 μm). However, in contrast to the SDS case, a third population, corresponding to droplets with a median size of about 15 μm, arose immediately. The volume of these larger droplets correspond to the combined volume of more than 200 of the smaller droplets with $d_m = \alpha_1$. The implication is that, in this case, the coalescence mode must involve local emulsion break down events. Large numbers of neighbouring droplets fuse at once to form a much larger droplet.

The oil droplets, in the freshly prepared emulsions, appeared similar irrespective of the surfactant used for stabilisation when observed under the microscope. Furthermore, there was no detectable change in the appearance of the emulsions stabilised with C12E4. The micrographs shown in Figure 11 confirms the development of larger droplets, over time, in the SDS and CTAB stabilised emulsions. It visualises the size of the droplets in as-prepared as well as in aged emulsions stabilised by 60 mM SDS and 50 mM CTAB respectively. The multimodal nature of the droplet sizes is clearly visible in the micrographs of the aged emulsions.

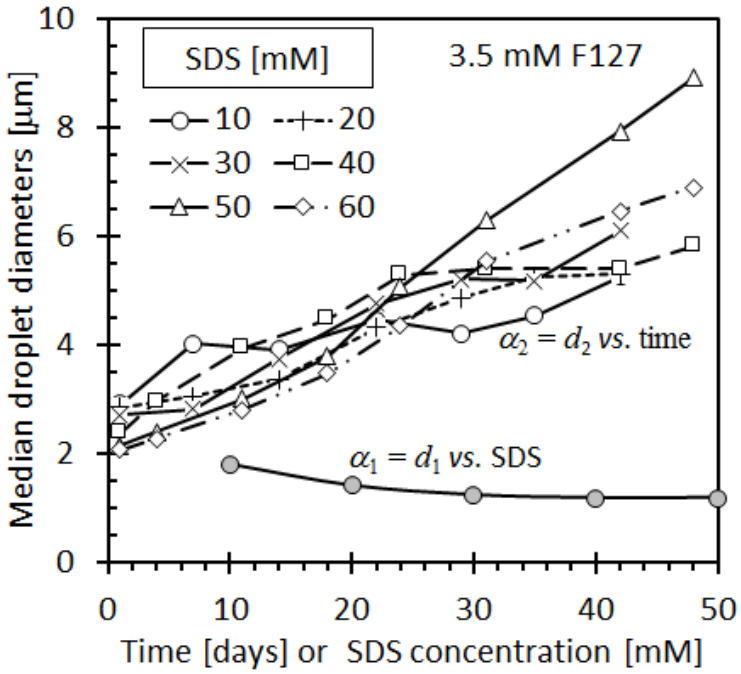

Figure 10. Trends in the mean particle size. The solid symbols show the dependence on SDS content on the median diameter for the lower size range droplets. The open symbols show the time-dependence of the median diameter of the higher range droplets.

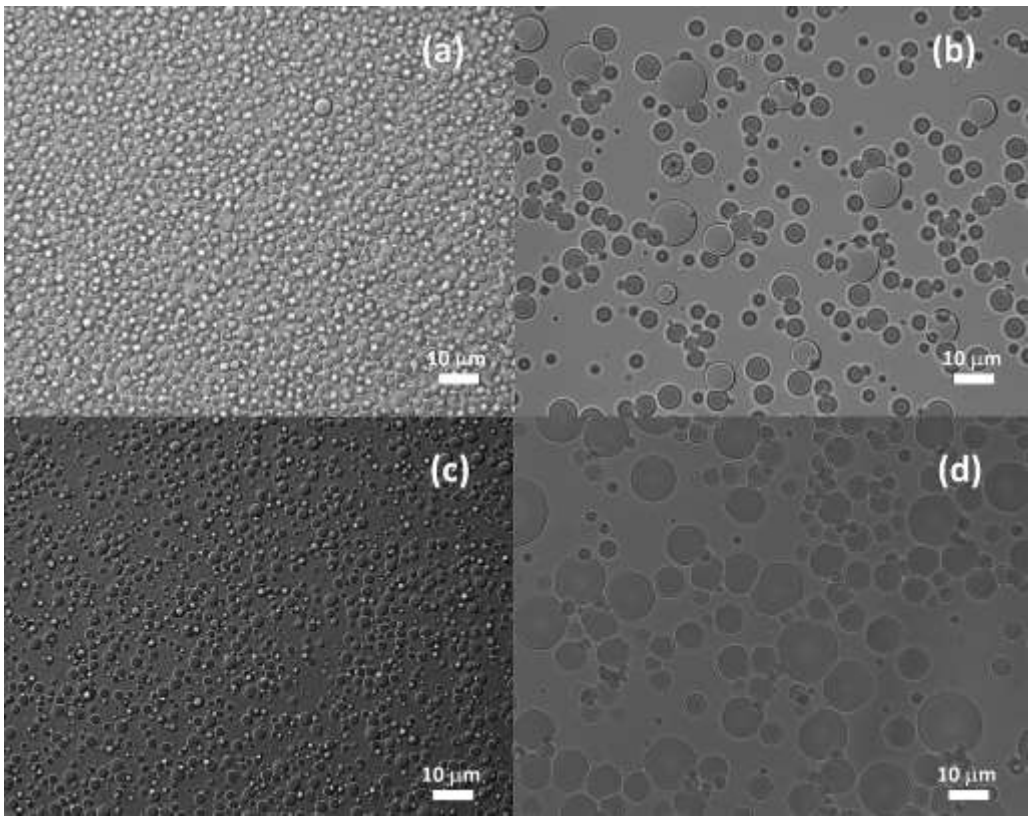

Figure 11. Optical micrographs of diluted emulsions containing either 60 mM SDS on (a) day 1 and (b) day 37, or 50 mM CTAB on (c) day 1 and (b) day 35. The dilution was 10× and 100× for the micrographs on the left and on the right respectively.

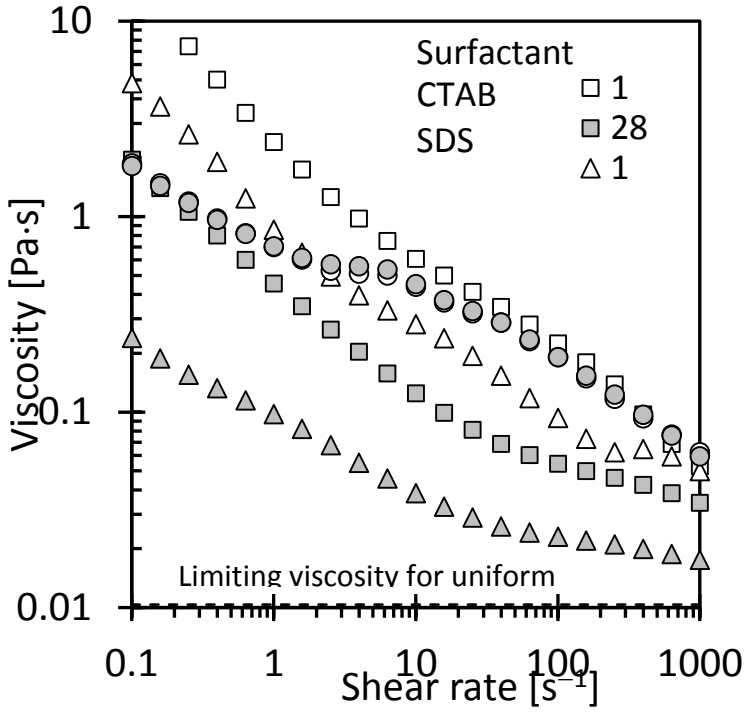

Figure 12. Representative viscosity vs. shear rate results obtained at 20°C. The emulsions contained 10 mM C12E4, 60 mM SDS or 50 mM CTAB in addition to 3.5 mM Pluronic F127. The flow curves were recorded on fresh emulsions and after ageing at 60°C.

Figure 12 shows representative data illustrating the effect of ageing on the viscosity of the emulsions as measured at 20°C. The emulsions all contained 3.5 mM Pluronic F127 together with 10 mM C12E4, 40 mM CTAB or 50 mM SDS. As expected, the viscosity data for the C12E4 stabilised emulsions did not change materially, even after ageing for 48 days at 60°C. Furthermore, the viscosity curves for all the C12E4 stabilised emulsions (5, 10, 20 or 30 mM C12E4) coincided. The viscosity was about 1.8 Pa·s at a shear rate of 0.1 s^{-1}. It rapidly decreased towards a narrow plateau region located in the shear rate window 2 to 6 Pa·s before decreasing again with increasing shear rate. The shape of this curve is consistent with expectations for highly concentrated emulsion [30]. Strong shear-thinning behaviour is observed prior to a yield stress, whereupon the intermediate pseudo-Newtonian behaviour is observed. Thereafter the structure rearranges and breaks (likely agglomerate breakdown and/or droplet deformation). The shape is similar, however the range of change of viscosity suggests that some other mechanism may be more prevalent; this is as of yet, unidentified. However, the present emulsions were not that concentrated. This might imply that the block copolymer was the determining factor controlling the emulsion viscosity. However, the reason for the anomalous flow curve shape is currently unknown.

At low shear rates, e.g. < 1 s^{-1}, the viscosity of the freshly prepared emulsions, stabilised with SDS or CTAB, featured even higher viscosities. The ranking, with respect to highest to lowest viscosity, was CTAB > SDS > C12E4. However, the viscosity curves for the emulsions stabilised with SDS or CTAB decreased more rapidly with increasing shear rate. There are hints of plateau regions at intermediate shear rates in the flow curves in Figure 12. They were quite distinctive in curves obtained for samples that experienced intermediate ageing times. At higher shear rates, the flow curves for SDS and CTAB stabilised emulsions lie below the one determined for the C12E4 stabilised emulsion.

The Newtonian viscosity of a suspension of non-interacting rigid spheres can be estimated with the following expression [31, 32]

$$\eta/\eta_o = \left(1-\varphi/\varphi_{\max}\right)^{-2.5\varphi_{\max}} \quad (3)$$

Where η and η_o are the viscosities of suspension and the neat liquid respectively; φ is the volume faction of the suspended spheres, and $\varphi_{\max}$ is the maximum random packing volume fraction of the suspended particles. For spheres with uniform size, $\varphi_{\max} \approx 0.64$. It is larger for particle size distributions. At 25°C the viscosity of water is about η = 0.91 mPa·s. This means that the viscosity for a dispersion of uniform, non-interacting spherical droplets present at a volume fraction of 50 vol-% is estimated to be about 0.0104 Pa·s. The viscosity of the neat, freshly prepared emulsions were about two orders of magnitude larger that this predicted value. This is consistent with significant droplet-droplet interactions leading to local emulsion structuring, in particular the formation of large droplet agglomerates. This turns them into rigid objects and they trap water in the interstices between the droplets. The trapped liquid becomes part of the dispersed phase, as it has to move with the rigid agglomerates. This means that less mobile liquid is available for fluid flow and that the effective volume fraction of the dispersed phase now exceeds the volume fraction of the stationary oil phase. Both effects lead to an increased emulsion viscosity as per equation (3). On application of sufficient shear, the local droplet structures are gradually broken down to smaller aggregates commensurate with the magnitude of the applied shear. When the agglomerates are reduced in size, part of the interstitial water is released. The amount of liquid available for flow is increased and the effective volume fraction of the dispersed phase is decreased. The end effect is a decrease in the viscosity, again as per the predictions

of equation (2). This explains the reduction in the emulsion viscosity as the shear rate is progressively increased.

The emulsion viscosity is expected to reach a low plateau at shear rates of sufficient magnitude to break all the agglomerates down to the point where all the droplets are free to move individually on their own. The lowest value recorded presently was 0.014 Pa·s obtained for an emulsion stabilised with 40 mM CTAB and measured at a shear rate of 100 s^{-1}. This is still higher than the value of 0.0104 Pa·s previously estimated. Actually, a free-flowing polydisperse emulsion should feature an even lower viscosity as the maximum random packing fraction would be higher than $\varphi_{max} = 0.64$. However, it should be noted that the effective volume fraction of emulsion droplets is actually somewhat higher than the volume fraction oil. This is because the surfactant chains extend into the water phase and in the process they effectively "solidify" a layer of water covering the surface of the oil droplet [32]. This increases the effective diameter of the oil droplets and thereby increases the effective volume fraction of the dispersed phase. Lastly, it is clear from Figure 12 that the viscosity curves were still trending downward toward an unknown viscosity plateau value.

Ageing lead to considerable changes in the flow curves for both the SDS and CTAB stabilised emulsions. The viscosity curves dropped to much lower values. They also asymptotically approach plateau values at high shear rates. This behaviour is also consistent with the notions that emulsions comprise droplet agglomerates and that droplet coalescence will affect and change their structure. For example, smaller droplets can occupy the gaps between larger drops. This reduces the interstitial space between the droplets. Therefore, the droplet coalescence process releases part of the liquid medium that was trapped and effectively "solidified". Simultaneously, the effective volume fraction of the dispersed phase decreases and the maximum random packing volume fraction φ_{max} increases. Once again, equation (3) indicates that the net effect will be a reduced viscosity. This explains why after some ageing the coalescing emulsions, based on the SDS and CTAB emulsifiers, eventually featured lower viscosities than the C12E4 stabilised emulsions.

4. Discussion

When all the results are considered together, the following picture emerges for emulsions stabilised with 3.5 mM Pluronic F127 combined with specified amounts of an anionic, a

cationic or a non-ionic surfactant. The high emulsion viscosity and its shear thinning behaviour is consistent with aggregation of the droplets yielding an emulsion in a near jammed state. Any liquid water trapped inside agglomerates is effectively immobilised and forms part of the dispersed phase. Applying some shear causes partial break down of the agglomerated structures releasing the interstitial water. The apparent viscosity decreases as the volume fraction of the continuous fluid is increased and the volume fraction of the effective dispersed phase is reduced. The breakdown process is progressive requiring sustained increase in shear for further reduction of droplet agglomerates in order to decrease the viscosity. Ultimately, a viscosity plateau is reached once all the droplets are free to move individually.

All freshly prepared emulsions already featured bimodal droplet size distributions. Pluronic F127-based emulsions stabilised with C12E4 as cosurfactant were the most stable, as the particle size distribution did not change even after ageing for 48 days at 60°C. Over time, those additionally based on SDS or CTAB evolved into multimodal distributions. The emulsion droplets belonging to the smaller size population did not coalesce with each other since the median diameter remained constant. However, they did merge with droplets from the larger-size population as their volume fraction decreased over time. In SDS stabilised emulsions the droplet size distribution corresponding to the larger particles shifted to larger diameters, indicative of coalescence events driven by binary droplet interactions. However, on ageing the evolution of the PSD of CTAB stabilised emulsions was characterised by the development of a new fractional distribution with a much higher median diameter rather than a progressive shift to larger particle diameters. This is consistent with coalescence dominated by cooperative events in which large numbers of droplets, about 200 or more, combined to form much larger droplets. It is likely that the coalescence events are linked to catastrophic local emulsion breakage at the droplet agglomerate level.

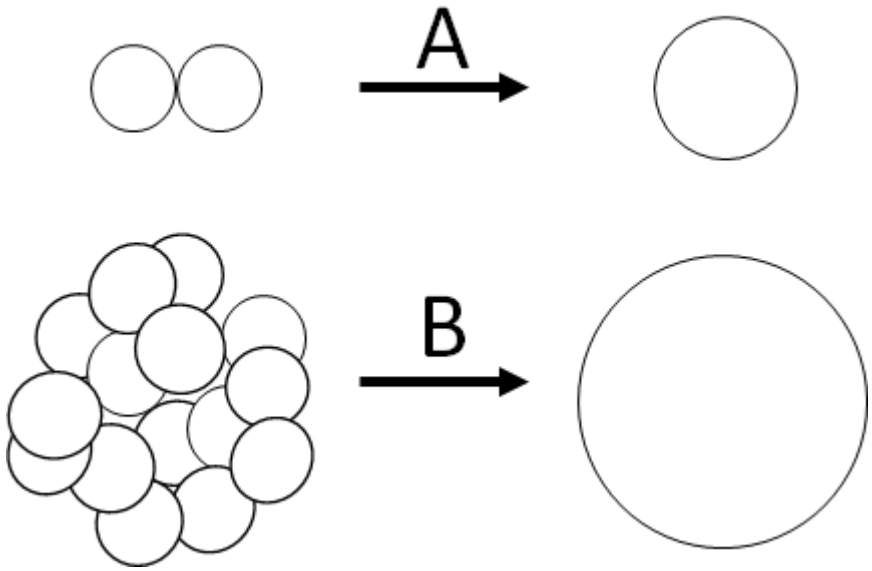

Scheme I. Coalescence mechanisms in (A) SDS, and (B) in CTAB stabilised emulsions

This suggests that the emulsion breakdown mechanisms in the two emulsions differed fundamentally. The behaviour of the SDS system is consistent with droplet coalescence mechanism (A) in Scheme I. However, the smaller droplets only coalesced with the larger droplets rather than with each other. That could explain the observation that their size remains constant but that their relative amount decreases over time.

With respect to the breaking mechanism for the CTAB-stabilised emulsion, breakage appears to occur according to mechanism (B) in Scheme I. In this scenario, numerous smaller aggregated droplets coalesce into larger droplets.

Conclusion

The stability of 50 vol-% mineral oil-in-water emulsions, in which the aqueous phase contained 0.37 M of Na_3PO_4 was studied. All freshly prepared emulsions already featured bimodal droplet size distributions. Emulsion stability was inferred from changes in the particle size distributions as a function of ageing at 60°C. Samples of the emulsions stabilised with the neat surfactants, e.g. 60 mM CTAB or 20 mM and C12E4 proved unstable breaking within one week. However, 50 mM SDS on its own was sufficient to yield a stable emulsion lasting for more than 48 days. Addition of 3.5 mM Pluronic F127 had little effect on the stability of the

SDS containing emulsion. However, it significantly improved the stability of the CTAB and C12E4 containing emulsions. This was especially true in the latter case as the emulsion prepared with 10 mM C12E4 as cosurfactant was very stable. Droplet size did not change over time, even after 48 days ageing at 60°C.

It was possible to deconvolute the multimodal droplet size distributions using linear combinations of series of log-logistic distributions. This analysis showed that, in all emulsions, the droplet population with the smallest size was stable with respect to the mean droplet diameter. However, the relative volume fraction decreased over time. This is consistent with the smaller droplets exclusively coalescing with large droplets. The observed shifts in droplet size with ageing time suggests two different coalescence mechanisms for the CTAB and SDS-stabilised emulsions. In the latter case, the coalescence is consistent with fusion events involving binary droplet interactions while in the former case the change is consistent with coordinated coalescence of large droplets assemblies in an abrupt fashion.

All the emulsions featured very high initial viscosities and strong shear thinning behaviour consistent with a jammed state for the emulsion droplets. Since the volume fraction of the dispersed phase was only 50 vol-%, this cannot be attributed merely to a geometric effect. It implies strong droplet-droplet interactions mediated by the block copolymer present. It is then possible to explain the high emulsion viscosity and the strong shear thinning effect by invoking the breakdown of large droplet agglomerates with increasing shear.

Acknowledgements

The authors express their gratitude to the University of Pretoria and the Institute of Applied Materials for a stipend to AK, the Council for Scientific and Industrial Research (CSIR) for allowing access to the surface tension instrument and to BASF for donation of the Pluronic F127 block copolymer.

References

[1] E. Hecht, H. Hoffmann, Kinetic and calorimetric investigations on micelle formation of block copolymers of the poloxamer type, Colloids and Surfaces A: Physicochemical and Engineering Aspects, 96 (1995) 181-197.
[2] P. Alexandridis, Poly(ethylene oxide)/poly(propylene oxide) block copolymer surfactants, Current Opinion in Colloid & Interface Science, 2 (1997) 478-489.
[3] P. Alexandridis, V. Athanassiou, S. Fukuda, T.A. Hatton, Surface Activity of Poly(ethylene oxide)-block-Poly(propylene oxide)-block-Poly(ethylene oxide) Copolymers, Langmuir, 10 (1994) 2604-2612.
[4] E. Hecht, H. Hoffmann, Interaction of ABA block copolymers with ionic surfactants in aqueous solution, Langmuir, 10 (1994) 86-91.
[5] G. Wanka, H. Hoffmann, W. Ulbricht, The aggregation behavior of poly-(oxyethylene)-poly-(oxypropylene)-poly-(oxyethylene)-block-copolymers in aqueous solution, Colloid & Polymer Science, 268 (1990) 101-117.
[6] P. Alexandridis, J.F. Holzwarth, T.A. Hatton, Micellization of Poly(ethylene oxide)-Poly(propylene oxide)-Poly(ethylene oxide) Triblock Copolymers in Aqueous Solutions: Thermodynamics of Copolymer Association, Macromolecules, 27 (1994) 2414-2425.
[7] M. Almgren, W. Brown, S. Hvidt, Self-aggregation and phase behavior of poly(ethylene oxide)-poly(propylene oxide)-poly(ethylene oxide) block copolymers in aqueous solution, Colloid & Polymer Science, 273 (1995) 2-15.
[8] P. Bahadur, Block copolymers – Their microdomain formation (in solid state) and surfactant behaviour (in solution), Current Science, 80 (2001) 1002-1007.
[9] T. Sottmann, Solubilization efficiency boosting by amphiphilic block co-polymers in microemulsions, Current Opinion in Colloid & Interface Science, 7 (2002) 57-65.
[10] K. Chari, B. Antalek, J. Kowalczyk, R.S. Eachus, T. Chen, Polymer-surfactant interaction and stability of amorphous colloidal particles, Journal of Physical Chemistry B, 103 (1999) 9867-9872.
[11] Y. Li, R. Xu, S. Couderc, M. Bloor, E. Wyn-Jones, J.F. Holzwarth, Binding of Sodium Dodecyl Sulfate (SDS) to the ABA Block Copolymer Pluronic F127 (EO97PO69EO97): F127 Aggregation Induced by SDS, Langmuir, 17 (2001) 183-188.
[12] R. Nagarajan, Thermodynamics of nonionic polymer—micelle association, Colloids and Surfaces, 13 (1985) 1-17.
[13] N.V. Sastry, H. Hoffmann, Interaction of amphiphilic block copolymer micelles with surfactants, Colloids and Surfaces A: Physicochemical and Engineering Aspects, 250 (2004) 247-261.
[14] S. Couderc-Azouani, J. Sidhu, T. Thurn, R. Xu, D.M. Bloor, J. Penfold, J.F. Holzwarth, E. Wyn-Jones, Binding of sodium dodecyl sulfate and hexaethylene glycol mono-n-dodecyl ether to the block copolymer L64: Electromotive force, microcalorimetry, surface tension, and small angle neutron scattering investigations of mixed micelles and polymer/micellar surfactant complexes, Langmuir, 21 (2005) 10197-10208.
[15] Y. Li, M. Bao, Z. Wang, H. Zhang, G. Xu, Aggregation behavior and complex structure between triblock copolymer and anionic surfactants, Journal of Molecular Structure, 985 (2011) 391-396.
[16] O. Ortona, G. D'Errico, L. Paduano, V. Vitagliano, Interaction between cationic, anionic, and non-ionic surfactants with ABA block copolymer Pluronic PE6200 and with BAB reverse block copolymer Pluronic 25R4, Journal of Colloid and Interface Science, 301 (2006) 63-77.
[17] J. Lunagariya, N.S. Kumar, M. Asif, A. Dhar, R.L. Vekariya, Dependency of Anion and Chain Length of Imidazolium Based Ionic Liquid on Micellization of the Block Copolymer F127 in Aqueous Solution: An Experimental Deep Insight, Polymers (Basel), 9 (2017) 285.
[18] Y. Zhang, Y.M. Lam, Study of Mixed Micelles and Interaction Parameters for Polymeric Nonionic and Normal Surfactants, Journal of Nanoscience and Nanotechnology, 6 (2006) 3877-3881.
[19] T. Thurn, S. Couderc, J. Sidhu, D.M. Bloor, J. Penfold, J.F. Holzwarth, E. Wyn-Jones, Study of mixed micelles and interaction parameters for ABA triblock copolymers of the type EOm-POn-EOm and ionic surfactants: Equilibrium and structure, Langmuir, 18 (2002) 9267-9275.

[20] P.R. Desai, N.J. Jain, R.K. Sharma, P. Bahadur, Effect of additives on the micellization of PEO/PPO/PEO block copolymer F127 in aqueous solution, Colloids and Surfaces A: Physicochemical and Engineering Aspects, 178 (2001) 57-69.
[21] Q. Jiang, Y.C. Chiew, J.E. Valentini, Adsorption of ethylene oxide/propylene oxide/ethylene oxide triblock copolymers at the air/water interface, Colloids and Surfaces A: Physicochemical and Engineering Aspects, 113 (1996) 127-134.
[22] C.A. Stan, S.K.Y. Tang, G.M. Whitesides, Independent Control of Drop Size and Velocity in Microfluidic Flow-Focusing Generators Using Variable Temperature and Flow Rate, Analytical Chemistry, 81 (2009) 2399-2402.
[23] C.C. Ruiz, Micelle formation and microenvironmental properties of sodium dodecyl sulfate in aqueous urea solutions, Colloids and Surfaces A: Physicochemical and Engineering Aspects, 147 (1999) 349-357.
[24] S.M. Alawi, Thermodynamics studies of cetyltrimethylammonium bromide (CTAB) in N, N-dimethyl acetamide-water mixtures, Oriental Journal of Chemistry, 26 (2010).
[25] J. Aguiar, P. Carpena, J.A. Molina-Bolívar, C. Carnero Ruiz, On the determination of the critical micelle concentration by the pyrene 1:3 ratio method, Journal of Colloid and Interface Science, 258 (2003) 116-122.
[26] Y. Li, R. Xu, D.M. Bloor, J.F. Holzwarth, E. Wyn-Jones, Binding of sodium dodecyl sulfate to the ABA block copolymer pluronic F127 (EO 97 PO 69 EO 97): An electromotive force, microcalorimetry, and light scattering investigation, Langmuir, 16 (2000) 10515-10520.
[27] Y. Li, M. Bao, Z. Wang, H. Zhang, G. Xu, Aggregation behavior and complex structure between triblock copolymer and anionic surfactants, Journal of Molecular Structure, 985 (2011) 391-396.
[28] Y. Li, R. Xu, S. Couderc, D.M. Bloor, J.F. Holzwarth, E. Wyn-Jones, Binding of tetradecyltrimethylammonium bromide to the ABA block copolymer Pluronic F127 (EO 97 PO 69 EO 97): Electromotive force, microcalorimetry, and light scattering studies, Langmuir, 17 (2001) 5742-5747.
[29] S. Couderc, Y. Li, D.M. Bloor, J.F. Holzwarth, E. Wyn-Jones, Interaction between the Nonionic Surfactant Hexaethylene Glycol Mono-n-dodecyl Ether (C12EO6) and the Surface Active Nonionic ABA Block Copolymer Pluronic F127 (EO97PO69EO97)Formation of Mixed Micelles Studied Using Isothermal Titration Calorimetry and Differential Scanning Calorimetry, Langmuir, 17 (2001) 4818-4824.
[30] S.R. Derkach, Rheology of emulsions, Advances in Colloid and Interface Science, 151 (2009) 1-23.
[31] I.M. Krieger, Rheology of monodisperse latices, Advances in Colloid and Interface Science, 3 (1972) 111-136.
[32] W.G.B. Mandersloot, K.J. Scott, Rheology of particle suspensions, South African Journal of Chemical Engineering, 2 (1990) 53-69.